

Loss of Imprinting of *Igf2* Alters Intestinal Maturation and Tumorigenesis in Mice

Takashi Sakatani,^{1*} Atsushi Kaneda,^{1*}
 Christine A. Iacobuzio-Donahue,^{2,3*} Mark G. Carter,⁵
 Sten de Boom Witzel,² Hideyuki Okano,⁶ Minoru S. H. Ko,⁵
 Rolf Ohlsson,⁷ Dan L. Longo,⁵ Andrew P. Feinberg^{1,3,4†}

Loss of imprinting (LOI) of the insulin-like growth factor II gene (*IGF2*) is an epigenetic alteration that results in a modest increase in IGF2 expression, and it is present in the normal colonic mucosa of about 30% of patients with colorectal cancer. To investigate its role in intestinal tumorigenesis, we created a mouse model of *Igf2* LOI by crossing female H19^{+/-} mice with male Apc^{+/-Min} mice. Mice with LOI developed twice as many intestinal tumors as did control littermates. Notably, these mice also showed a shift toward a less differentiated normal intestinal epithelium, reflected by an increase in crypt length and increased staining with progenitor cell markers. A similar shift in differentiation was seen in the normal colonic mucosa of humans with LOI. Thus, altered maturation of nonneoplastic tissue may be one mechanism by which epigenetic changes affect cancer risk.

Genomic imprinting is a parent-of-origin gene-silencing mechanism thought to be important in growth regulation. Loss of imprinting (LOI) of the human insulin-like growth factor II gene (*IGF2*), or activation of the normally silent maternally inherited allele, occurs in many common cancers (1). About 10% of the population shows LOI of *IGF2*, and this molecular trait is associated with a personal and/or family history of colorectal neoplasia (2, 3).

To investigate the mechanism by which LOI of *IGF2* contributes to intestinal tumorigenesis, we created a mouse model. Previous analyses of mouse models by other groups have shown that *Igf2* is activated more than 25-fold in pancreatic tumors induced by the SV40 large T antigen (4) and that forced overexpression of *Igf2* causes intestinal tumor formation and hyperproliferation of crypt epithelium (5, 6). Our model was designed to more closely mimic the human situation, where LOI causes only a modest increase in *IGF2* expression. We took advantage of the fact that imprinting of *Igf2* is regulated by a

differentially methylated region (DMR) upstream of the nearby untranslated *H19* gene. Deletion of the DMR leads to biallelic expression (LOI) of *Igf2* in the offspring when the deletion is maternally inherited (7–9) (fig. S1). To model intestinal neoplasia, we used *Min* mice with an *Apc* mutation (10). We crossed female H19^{+/-} with male Apc^{+/-Min}, comparing littermates harboring *Apc* mutations with or without a maternally inherited *H19* deletion, and thus with or without LOI. In comparison with H19^{+/+} [hereafter referred to as LOI(–) mice], the H19^{+/-} mutant mice [hereafter referred to as LOI(+) mice] showed an approximate doubling in *Igf2* mRNA levels that did not vary with age or *Min* status (fig. S2). This is consistent with the two- to threefold increase in *Igf2* mRNA levels in normal human colonic mucosa or Wilms tumors that are LOI(+) (3, 11). The amount of Igf2 protein was also doubled in

the intestine of LOI(+) mice (fig. S2). The LOI(+) mice developed about twice as many adenomas in both small intestine and colon as did the LOI(–) mice, and this difference was statistically significant (Table 1). Mice with LOI also had longer intestinal crypts, the site of epithelial stem cell renewal (12, 13) (fig. S3). This increase in length was specific to the crypts, progressed over time [1.2-fold increase ($P < 0.01$) in mice at 42 days of age and 1.5-fold increase ($P < 0.0001$) in mice at 120 days], and was independent of *Apc* status. The increase in crypt length was not due to differences in cell proliferation, because there was no statistically significant difference in proliferating cell nuclear antigen labeling index between LOI(+) and LOI(–) *Min* mice (3.8 ± 0.9 versus 3.1 ± 1.5 , respectively), nor was there a difference in the distribution (14) of proliferative cells within the crypt (0.39 ± 0.04 versus 0.38 ± 0.03 , respectively; $P =$ not significant). The LOI(+) and LOI(–) mice showed no difference in crypt apoptotic rates, as assessed histomorphologically and by in situ terminal deoxynucleotidyl transferase-mediated dUTP nick-end labeling (TUNEL); both genotypes had an average of 1 apoptotic cell per 20 crypts. There was also no difference in the rate of branching of intestinal crypts; both LOI(+) and LOI(–) mice had one or two total branched crypts below the intestinal surface.

We hypothesized that the increase in crypt length of the small intestine was due to a shift in the ratio of undifferentiated to differentiated epithelial cells in the mucosa. To test this, we immunostained for four antigens that mark undifferentiated versus differentiated epithelial cell development: villin, a structural component of the brush border cytoskeleton in gastrointestinal tract epithelia (15); ephrin-B1, the ligand of the EphB2/EphB3 receptors that play a role in allocating epithelial cells within the crypt-villus axis in intestinal epithelium (16); musashi1, an RNA-binding protein selectively expressed in neural and intestinal progenitor cells and key to

Table 1. Increased adenoma number and surface area in LOI(+) *Min* mice. Displayed are the adenoma counts, as well as counts corrected for intestinal surface area alone or for both intestinal and adenoma surface area. Values are given as the mean \pm SE; P value was calculated by Student's t test.

| Genotype | <i>N</i> | Small intestine | Fold increase; <i>P</i> value | Colon | Fold increase; <i>P</i> value |
|---|----------|-----------------|-------------------------------|---------------|-------------------------------|
| <i>Number of adenomas</i> | | | | | |
| LOI(–) <i>Min</i> | 81 | 27.7 \pm 1.3 | 2.2; | 1.3 \pm 0.1 | 2.2; |
| LOI(+) <i>Min</i> | 59 | 60.4 \pm 3.7 | <0.00001 | 2.9 \pm 0.3 | <0.0001 |
| <i>Surface area of adenomas (% of intestine occupied by adenomas)</i> | | | | | |
| LOI(–) <i>Min</i> | 81 | 2.2 \pm 0.1 | 2.4; | 2.3 \pm 0.3 | 2.5; |
| LOI(+) <i>Min</i> | 59 | 5.5 \pm 0.4 | <0.00001 | 5.8 \pm 0.9 | <0.001 |
| <i>Number of adenomas/10 cm² of intestine</i> | | | | | |
| LOI(–) <i>Min</i> | 81 | 10.8 \pm 0.5 | 1.8; | 3.7 \pm 0.5 | 1.9; |
| LOI(+) <i>Min</i> | 59 | 19.2 \pm 1.1 | <0.00001 | 7.0 \pm 0.8 | <0.0001 |

¹Department of Medicine, ²Department of Pathology, ³Oncology Center, ⁴Department of Molecular Biology and Genetics, Johns Hopkins University School of Medicine, Baltimore, MD 21205, USA. ⁵Laboratory of Genetics, National Institute on Aging, National Institutes of Health, Baltimore, MD 21224, USA. ⁶Department of Physiology, Keio University School of Medicine, Tokyo 160-8582, Japan. ⁷Department of Development and Genetics, Uppsala University, S-752 36 Uppsala, Sweden.

*These authors contributed equally to this work.
 †To whom correspondence should be addressed.
 E-mail: afeinberg@jhu.edu

maintaining the stem cell state (17, 18); and twist, a transcriptional factor of the basic helix-loop-helix family originally identified as a mesodermal progenitor cell marker (19) that is also involved in loss of differentiation of epithelial cells (20, 21).

Consistent with their biological roles in differentiated enterocytes, immunostaining for both villin and ephrin-B1 was detected within the cytoplasm of enterocytes lining the villi of the small intestine and within the villus-crypt interface in LOI(-) mice (Fig. 1A, fig. S4). The LOI(+) mice, in contrast, showed lower levels of villin and ephrin-B1 and a contraction of the differentiated epithelial cell compartment (Fig. 1B, fig. S4).

Expression of the progenitor cell marker musashi1 was observed in scattered cells within the lower half of intestinal crypts in LOI(-) mice (Fig. 1C), whereas numerous musashi1-positive cells were identified within the intestinal crypts of LOI(+) mice (Fig. 1D). The LOI(+) mice also showed intense staining within enterocytes lining the intestinal villi compared with LOI(-) mice (Fig. 1, E

and F). A semiquantitative analysis confirmed increased musashi1 staining in the LOI(+) mice, independent of *Apc* status (table S1). Immunostaining for twist also revealed a marked increase in the number and intensity of positively staining cells in the crypts of LOI(+) mice (fig. S5). These changes were progressive over time (Fig. 1, figs. S4 and S5).

Because this shift affects normal mucosa, one prediction of this dedifferentiation model is that the increased number of adenomas is due to an increase in tumor initiation rather than an increase in tumor progression. Supporting this idea, there was no difference in the ratio of microadenomas [<5 crypts each (22)] to macroadenomas (≥ 5 crypts each) between LOI(+) Min mice (36 micro-/27 macroadenomas) and LOI(-) Min mice (16 micro-/14 macroadenomas) at 120 days. An independent mouse model of LOI, in which point mutations had been introduced in three of the four CCCTC-binding factor (CTCF) target sites within the *H19* DMR (23) (figs. S1 and S6), was also examined by immunostaining. Another advantage of this model

is that, unlike the deletion model, *H19* expression is intact in the DMR mutation model (fig. S7). Loss of *H19* might have independent effects given its known role in mRNA translation in trans (24). Nevertheless, a shift in the ratio of differentiated to undifferentiated cells was also seen in the normal epithelium of these LOI(+) mice (Fig. 2, A to D, shows immunohistochemical staining for musashi1 and villin in colon epithelium).

Finally, we compared the normal mucosa of patients requiring biopsy during colonoscopic screening, whose LOI status was previously determined (2). No morphological differences were noted by conventional microscopy. However, 10 of 11 patients with LOI in the colon showed increased musashi1 staining extending to the upper half of colonic crypts and/or surface epithelium, compared with 5 of 15 patients without LOI ($P = 0.004$, Fisher's exact test) (Fig. 2, E and F; fig. S8). Altered colon epithelial maturation was also found in all four patients with LOI restricted to the colon ($P = 0.03$) and in six of seven patients with LOI in both peripheral blood lymphocytes and colon ($P = 0.03$), compared with patients without LOI.

The sensitivity was reduced but the specificity increased when musashi1 staining was combined with a second marker, twist; increased staining was seen in 6 of 11 patients with LOI, compared with 1 of 14 patients without LOI ($P = 0.02$, Fisher's exact test) (Fig. 2, G and H). Although twist staining alone did not attain statistical significance ($P = 0.07$), the two markers were nonoverlapping, suggesting heterogeneity in the downstream effects of LOI.

In summary, this study suggests a cellular mechanism by which epigenetic alterations in normal cells may affect cancer risk, namely, by altering the balance of differentiated and undifferentiated cells. The epigenetically mediated shift in normal tissue to a more undifferentiated state, as described here, might increase the target cell population for subsequent genetic alterations or might act alone in tumor initiation. In LOI-mediated Wilms tumor in the rare disorder Beckwith-Wiedemann syndrome (BWS), tumors arise because of an expanded population of nephrogenic precursor cells (25). We observed pancreatic islet cell hyperplasia, a feature of BWS, in LOI(+) Min mice (26), suggesting that LOI may also predispose to the development of other tumor types. Genetic mechanisms that alter cell differentiation and/or disrupt crypt architecture have been described (27–30), although these mechanisms are not common in normal human tissue. Whether the shift in epithelial maturation is a more specific predictor of cancer risk than LOI itself is an important question that will require studies of large numbers of patients using more molecular markers.

Fig. 1. Immunohistochemical analysis of villin and musashi1 in 120-day-old LOI(-) and LOI(+) mice. (A) In LOI(-) mice, villin protein expression is noted in a cytoplasmic distribution throughout differentiated enterocytes lining intestinal villi and within the crypt-villus interface. (B) In LOI(+) mice, villin expression is markedly decreased. (C) In LOI(-) mice, musashi1 expression is detected within the cytoplasm and nuclei in rare cells within intestinal crypts (arrow), the location of intestinal stem cells and the undifferentiated epithelial cell compartment. (D) In marked contrast, musashi1 cytoplasmic and nuclear labeling is detected throughout the intestinal crypts of LOI(+) mice. (E) In LOI(-) mice, rare musashi1-positive cells are detected within the overlying intestinal villi representing the differentiated epithelial compartment. (F) In LOI(+) mice, intense cytoplasmic and nuclear expression of musashi1 is detected within enterocytes lining intestinal villi. Bars, 10 μ m.

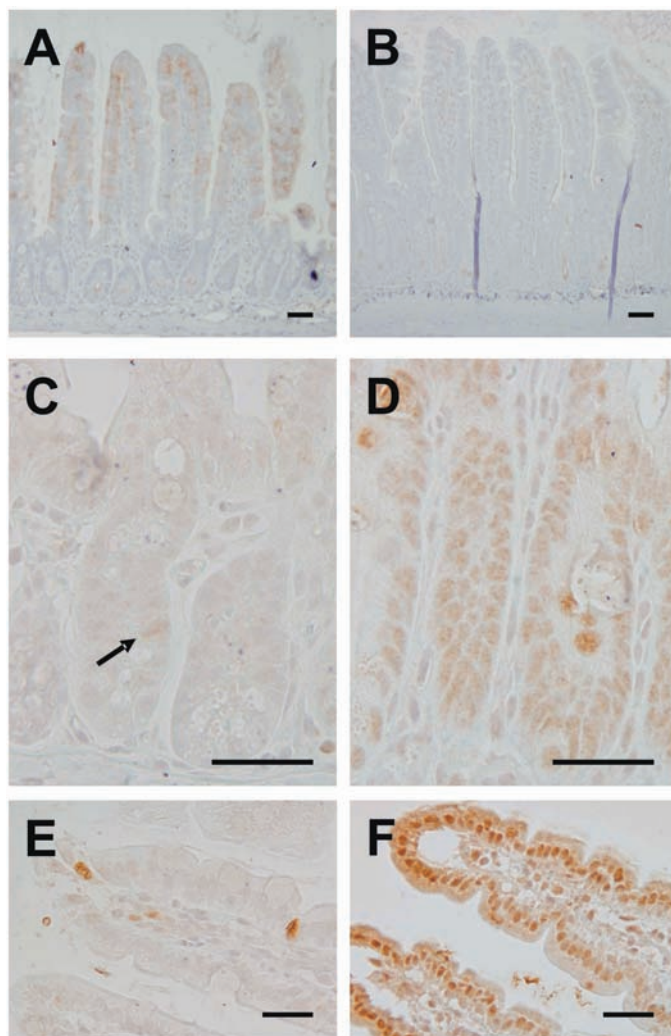
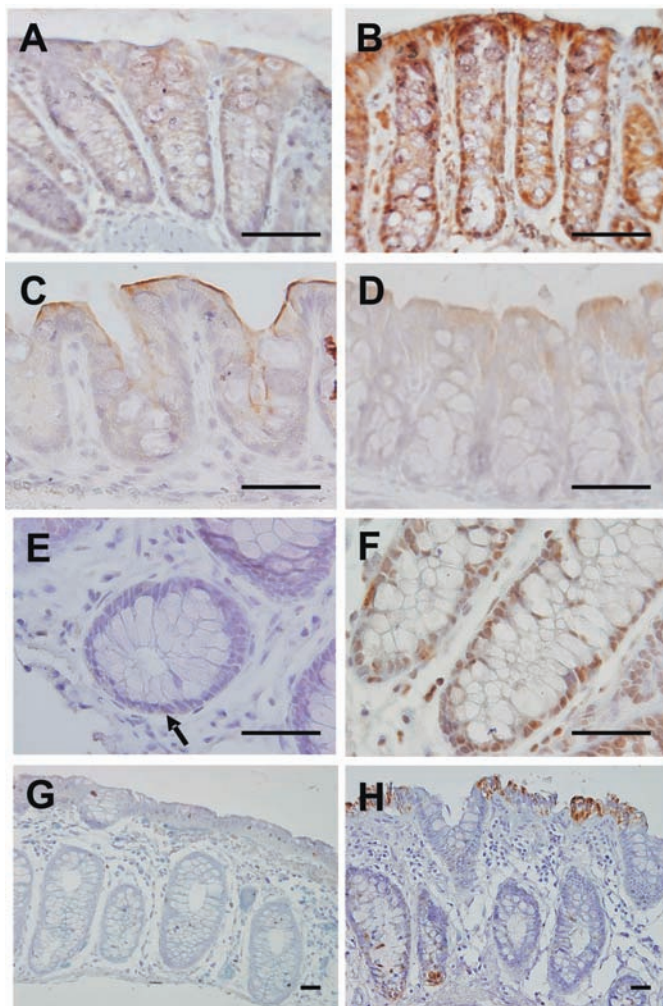


Fig. 2. A shift to less differentiated colon epithelium in a mouse *H19* DMR mutation model and in colonoscopy patients with LOI. (A) Musashi1 immunostaining in LOI(−) mice shows rare crypt epithelial cells with cytoplasmic labeling. (B) In contrast, LOI(+) mice show aberrant musashi1 staining in both a cytoplasmic and nuclear pattern throughout the colonic epithelium. (C) Villin immunostaining in LOI(−) mice shows cytoplasmic labeling that includes the brush border. (D) In contrast, in LOI(+) mice, villin staining of the brush border on the surface epithelial cells is absent. (E) In colonoscopy patients without LOI, rare musashi1-positive cells are detected in crypt epithelial cells (arrow). Low-power view is available in fig. S8. (F) In contrast, in colonoscopy patients with LOI, musashi1 labeling is present throughout colonic crypts and extends to the surface epithelium (see also fig. S8). (G) In colonoscopy patients without LOI, only weak labeling for twist is detected. (H) In colonoscopy patients with LOI, patchy but strong twist labeling is present in the crypt and surface epithelium. Bars, 10 μm.



References and Notes

1. A. P. Feinberg, *Semin. Cancer Biol.* **14**, 427 (2004).
2. H. Cui *et al.*, *Science* **299**, 1753 (2003).
3. K. Woodson *et al.*, *J. Natl. Cancer Inst.* **96**, 407 (2004).

4. G. Christofori, P. Naik, D. Hanahan, *Nat. Genet.* **10**, 196 (1995).
5. A. B. Hassan, J. A. Howell, *Cancer Res.* **60**, 1070 (2000).
6. W. R. Bennett, T. E. Crew, J. M. Slack, A. Ward, *Development* **130**, 1079 (2003).

7. P. A. Leighton, R. S. Ingram, J. Eggenschwiler, A. Efstratiadis, S. M. Tilghman, *Nature* **375**, 34 (1995).
8. M. A. Ripoche, C. Kress, F. Poirier, L. Dandolo, *Genes Dev.* **11**, 1596 (1997).
9. Materials and methods are available as supporting material on Science Online.
10. L. K. Su *et al.*, *Science* **256**, 668 (1992).
11. J. D. Ravenel *et al.*, *J. Natl. Cancer Inst.* **93**, 1698 (2001).
12. S. Sell, G. B. Pierce, *Lab. Invest.* **70**, 6 (1994).
13. G. H. Segal, R. E. Petras, in *Histology for Pathologists*, S. S. Sternberg, Ed. (Lippincott-Raven, Philadelphia, 1997), pp. 495–518.
14. M. Lipkin, E. Deschner, *Cancer Res.* **36**, 2665 (1976).
15. A. B. West *et al.*, *Gastroenterology* **94**, 343 (1988).
16. E. Battle *et al.*, *Cell* **111**, 251 (2002).
17. Y. Kaneko *et al.*, *Dev. Neurosci.* **22**, 139 (2000).
18. C. S. Potten *et al.*, *Differentiation* **71**, 28 (2003).
19. O. M. Borkowski, N. H. Brown, M. Bate, *Development* **121**, 4183 (1995).
20. L. R. Howe, O. Watanabe, J. Leonard, A. M. Brown, *Cancer Res.* **63**, 1906 (2003).
21. J. P. Thiery, M. Morgan, *Nat. Med.* **10**, 777 (2004).
22. C. J. Torrance *et al.*, *Nat. Med.* **6**, 1024 (2000).
23. V. Pant *et al.*, *Genes Dev.* **17**, 586 (2003).
24. Y. M. Li *et al.*, *J. Biol. Chem.* **273**, 28247 (1998).
25. J. B. Beckwith, N. B. Kiviat, J. F. Bonadio, *Pediatr. Pathol.* **10**, 1 (1990).
26. T. Sakatani *et al.*, data not shown.
27. A. P. Haramis *et al.*, *Science* **303**, 1684 (2004).
28. M. van de Wetering *et al.*, *Cell* **111**, 241 (2002).
29. W. Yang, L. Bancroft, C. Nicholas, I. Lozonschi, L. H. Augenlicht, *Cancer Res.* **63**, 4990 (2003).
30. A. Velcich *et al.*, *Science* **295**, 1726 (2002).
31. We thank S. Tilghman for the H19 deletion mouse strain, A. Hershfeld for technical assistance, and B. Vogelstein, E. Fearon, B. Beckwith, R. Hruban, and A. Sawa for helpful discussions. Supported by NIH grants R01CA65145 (A.P.F.), K08CA106610 (C.A.I.-D.), a Uehara Memorial Foundation grant (A.K.), and the Swedish Cancer Research Foundation (R.O.). The Johns Hopkins University and the NIH have filed a provisional patent application on the LOI mouse cancer model and immunohistochemical marker use. A.P.F. is a paid consultant to Epigenomics AG.

Supporting Online Material

www.sciencemag.org/cgi/content/full/1108080/DC1
 Material and Methods
 Figs. S1 to S8
 Table S1
 References

30 November 2004; accepted 13 January 2005
 Published online 24 February 2005;
 10.1126/science.1108080
 Include this information when citing this paper.

Turn a new page to...

www.sciencemag.org/books

Science
Books et al.
 HOME PAGE

- ▶ the latest book reviews
- ▶ extensive review archive
- ▶ topical books received lists
- ▶ buy books online